university of groningen

University Medical Center Groningen

University of Groningen

Resonant tunneling through the triple-humped fission barrier of U-236

Csatlos, M; Krasznahorkay, A; Thirolf, PG; Habs, D; Eisermann, Y; Faestermann, T; Graw, G; Gulyas, J; Harakeh, MN; Hertenberger, R

Published in:
Physics Letters B

DOI:
10.1016/j.physletb.2005.04.042

IMPORTANT NOTE: You are advised to consult the publisher's version (publisher's PDF) if you wish to cite from it. Please check the document version below.

Document Version
Publisher's PDF, also known as Version of record

Publication date:
2005

Link to publication in University of Groningen/UMCG research database

Citation for published version (APA):
Csatlos, M., Krasznahorkay, A., Thirolf, PG., Habs, D., Eisermann, Y., Faestermann, T., ... Wirth, HF. (2005). Resonant tunneling through the triple-humped fission barrier of U-236. Physics Letters B, 615(3-4), 175-185. https://doi.org/10.1016/j.physletb.2005.04.042

Copyright
Other than for strictly personal use, it is not permitted to download or to forward/distribute the text or part of it without the consent of the author(s) and/or copyright holder(s), unless the work is under an open content license (like Creative Commons).

Take-down policy
If you believe that this document breaches copyright please contact us providing details, and we will remove access to the work immediately and investigate your claim.

Downloaded from the University of Groningen/UMCG research database (Pure): http://www.rug.nl/research/portal. For technical reasons the number of authors shown on this cover page is limited to 10 maximum.

Download date: 21-05-2019

Available online at www.sciencedirect.com
SCIENCE DIRECT®
Physics Letters B 615 (2005) 175–185
PHYSICS LETTERS B
www.elsevier.com/locate/physletb

Resonant tunneling through the triple-humped fission barrier of ^{236}U

M. Csatlós [a], A. Krasznahorkay [a], P.G. Thirolf [b], D. Habs [b], Y. Eisermann [b], T. Faestermann [c], G. Graw [b], J. Gulyás [a], M.N. Harakeh [d], R. Hertenberger [b], M. Hunyadi [a,d], H.J. Maier [b], Z. Máté [a], O. Schaile [b], H.-F. Wirth [b]

[a] *Institute of Nuclear Research of the Hungarian Academy of Sciences, P.O. Box 51, H-4001 Debrecen, Hungary*
[b] *Department für Physik, Universität München, D-85748 Garching, Germany*
[c] *Technische Universität München, D-85748 Garching, Germany*
[d] *Kernfysisch Versneller Instituut, 9747 AA Groningen, The Netherlands*

Received 21 August 2004; received in revised form 14 March 2005; accepted 19 April 2005

Available online 28 April 2005

Editor: V. Metag

Abstract

The fission probability of ^{236}U as a function of the excitation energy has been measured with high energy resolution using the ^{235}U(d, pf) reaction in order to study hyperdeformed (HD) rotational bands. Rotational band structures with a moment of inertia of $\theta = 217 \pm 38\ \hbar^2$/MeV have been observed, corresponding to hyperdeformed configurations. From the level density of the rotational bands the excitation energy of the ground state in the third minimum was determined to be 2.7 ± 0.4 MeV.

The excitation energy of the lowest hyperdeformed transmission resonance and the energy dependence of the fission isomer population probability enabled the determination of the height of the inner fission barrier $E_A = 5.05 \pm 0.20$ MeV and its curvature parameter $\hbar\omega_A = 1.2$ MeV. Using this new method the long-standing uncertainties in determining the height of the inner potential barrier in uranium isotopes could be resolved.
© 2005 Elsevier B.V. All rights reserved.

PACS: 21.10.Re; 24.30.Gd; 25.85.Ge; 27.90.+b

1. Introduction

The study of nuclei with exotic shapes (super- and hyperdeformation) is one of the most vital fields in modern nuclear structure physics. Superdeformed (SD) nuclei in the second minimum have shapes with an axis ratio (c/a) of about 2 : 1, whilst hyperdeformed (HD) nuclei in the third minimum correspond to even more elongated shapes with axis ratio (c/a) of about 3 : 1 [1,2]. This is where the nucleus ^{236}U is exceptional, because it is the only isotope where hyperde-

E-mail address: peter.thirolf@physik.uni-muenchen.de (P.G. Thirolf).

0370-2693/$ – see front matter © 2005 Elsevier B.V. All rights reserved.
doi:10.1016/j.physletb.2005.04.042

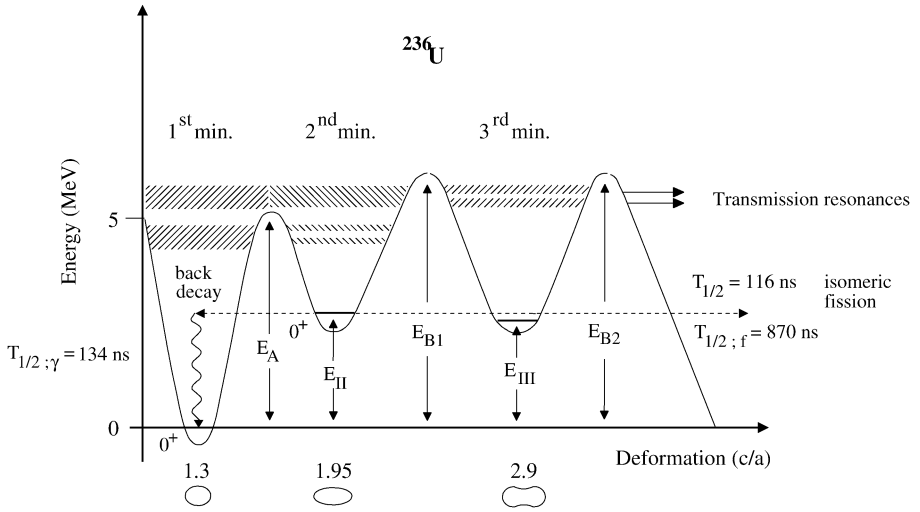

Fig. 1. The triple-humped potential-energy surface of ^{236}U. Also damped class-I, class-II and class-III compound states are shown in the three minima. For strongly mixed class-I and class-II states, transmission resonances of class-III states can occur in fission.

formed transmission resonances have been observed [3] and at the same time a superdeformed fission isomer is well-established [4]. Fig. 1 schematically shows the potential-energy surface (PES) of ^{236}U as a function of deformation (axis ratio) with the triple-humped fission barrier as deduced in this publication. Prominent new features are the lower inner barrier E_A and the large depth of the third minimum $(E_{B1}+E_{B2})/2-E_{\mathrm{III}}$. All peaks of the barriers are saddle points in a multi-dimensional deformation space [5].

Starting from this general picture we first focus on the properties of the third minimum. The presence of a third minimum in the fission barrier of light actinides, obtained from PES calculations, was first proposed by Möller and Nix [5,6]. According to more recent calculations, the third minimum in these nuclei appears at large quadrupole ($\beta_2 \sim 0.9$) and octupole deformations ($\beta_3 \sim 0.35$) and the depth is predicted to be much larger than previously believed [7]. Since these hyperdeformed actinide nuclei are also octupole deformed with reflection-asymmetric shapes, they show a possible energy splitting between different parity members of the rotational bands. The third minimum was first established experimentally for thorium nuclei, studying the microstructure in transmission resonances with (n, f), (t, pf) and (d, pf) reactions [8,9]. For hyperdeformed transmission resonances to occur it is necessary that the class-I and class-II compound states are strongly mixed. Otherwise, the narrow class-II states in general will not overlap with the isolated class-III states. The well-established idea of transmission resonances in the second minimum [10] could be carried over to the third minimum for mixed class-I and class-II states by simply replacing the former resonant class-II states by new resonant class-III states. The previous penetrabilities P_A and P_B now can be replaced by P_{B1} and P_{B2} corresponding to the two barriers enclosing the third minimum.

Hyperdeformed resonances were also observed in uranium isotopes [3,11]. In a previous measurement we identified three transmission-resonance groups at 5.27, 5.34 and 5.43 MeV in ^{236}U as groups of hyperdeformed $K = 4$ bands [3]. Although the energy resolution was limited to 20 keV and individual members of the rotational bands could not be resolved, a rotational parameter $\hbar^2/2\theta = 1.6^{+1.0}_{-0.4}$ keV was determined in good agreement with the value predicted for a hyperdeformed state $\hbar^2/2\theta_{\mathrm{theor}} = 2.0$ keV. In the new measurement we achieved an energy resolution of ≈ 5 keV and were able to resolve the individual members of the rotational bands. For a group of lower transmission resonances around 5.1 MeV, which formerly was assumed to be a transmission resonance in the second minimum, a good fit of fission probability and angular correlation data could only be obtained by assigning it to a transmission resonance in the third minimum. The observation of rotational bands in the third minimum requires a rather complete damping of

states in the second minimum and thus allows to determine an upper limit for the inner-barrier height E_A. Combining this with results from the fission-isomer population probability [12,13], we can for the first time now determine the inner barrier height in ^{236}U, where formerly values differing by 1 MeV were obtained. The uncertainty in the height of the inner barrier occurs for all light actinides and was called the 'thorium anomaly' [4] as it was first observed in thorium nuclei. It is now resolved in the picture of the triple-humped barrier and we reach a much better understanding of the potential-energy landscape of light actinides in agreement with more recent predictions [7,14].

2. Experimental method

The experiment was carried out at the Munich Accelerator Laboratory. We investigated the ^{235}U$(d, pf)^{236}$U reaction in the excitation energy range $4.9 < E^* < 5.6$ MeV. The deuteron beam energy was $E_d = 9.73$ MeV. An enriched (99.89%), 88 μg/cm^2 thick target of $^{235}U_2O_3$ on a 30 μg/cm^2 thick carbon backing was used.

The excitation energy of the ^{236}U compound nucleus can directly be deduced from the kinetic energy of the outgoing protons. The ground state Q-value for the ^{235}U$(d, p)^{236}$U reaction is $Q_{GS} = 4.320 \pm 0.002$ MeV, which was calculated using the NuBase Q-value calculator [15], based on the atomic mass data taken from the compilation by Audi and Wapstra [16,17].

The kinetic energy of the proton ejectiles was analyzed with a Q3D magnetic spectrometer [18] placed at $\Theta_L = 125°$ relative to the incident beam, covering a solid angle of 10 msr. The position of the analyzed particles in the focal plane was measured with a position-sensitive light-ion focal plane detector with individual cathode strip readout of 890 mm active length [19]. The ^{208}Pb(d, p) reaction ($Q = 1.712 \pm 0.004$ MeV) was used for the energy calibration. Using an identical magnetic field setting as in the case of the (d, p) reaction on uranium the $E^* = 2537$ keV and $E^* = 2492$ keV transitions in ^{209}Pb provided the energy calibration. The position and width of these lines were repeatedly checked during the measurement, proving the stability of the energy calibration. The energy resolution obtained from the ^{208}Pb(d, p) reaction using a thin target (57 μg/cm^2 on a 7 μg/cm^2 carbon backing) was 3 keV (FWHM) at 8.7 MeV proton energy. Due to the different target properties and the longterm drifts during the one week measurement time an experimental energy resolution of about 5 keV (FWHM) can be estimated for the ^{235}U(d, pf) reaction. It is mainly due to this excellent resolution that qualitatively new information could be extracted from an already well-studied reaction. Fission fragments were detected in coincidence with the outgoing protons by two parallel plate avalanche counters (PPAC) [20] with active areas of 16×16 cm^2, each positioned in a distance of 23 cm from the target, covering a solid angle of about 4% and an angular range of $55 \pm 20°$ and $125 \pm 20°$ relative to the beam direction (corresponding to 65°–90° relative to the recoil axis). This limitation in angular coverage resulted from an optimization of the setup for time-of-flight rather than for angular correlation measurements thus preventing the extraction of angular correlation information from the present data. During 100 hours 2.6×10^5 proton-fission coincidence events were acquired at typical count rates of 200/s for the focal plane detector and 1×10^4/s for the fission counters. As identified from the proton-fission coincidence timing spectrum the ratio between real and random events amounted to $\approx 4:1$ in average for the whole spectrum. Contributions from random coincidences were subtracted from the proton data.

3. Experimental results and discussion

The excitation energy spectrum derived from the proton kinetic energies measured in coincidence with the fission fragments following the ^{235}U(d, pf) reaction is shown in Fig. 2.

The measured high-resolution fission probability is shown in Fig. 3(a) as a function of the excitation energy of the compound nucleus ^{236}U. It was obtained by dividing the proton energy spectrum measured in coincidence with fission fragments by the smoothly varying proton spectrum from the (d, p) reaction.

Fig. 3(c) in comparison shows the same fission probability of ^{236}U measured by Just et al. [13] with a $\Delta E - E$ telescope for the light particles, reaching an energy resolution of 80 keV. This measurement covered a broader range of excitation energies, its energy

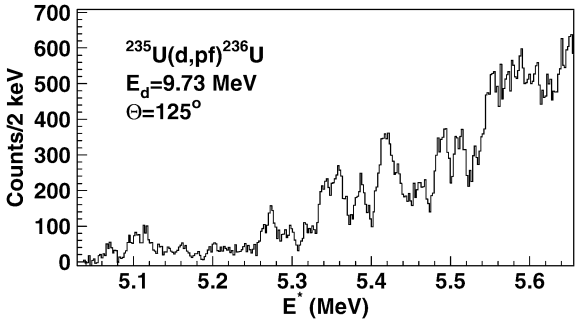

Fig. 2. Excitation energy spectrum inferred from the proton kinetic energies following the ^{235}U(d, pf) reaction measured in coincidence with the fission fragments.

calibration agrees within 20 keV with the present measurement. From the angular distribution of the fission fragments the angular correlation coefficient A_2 was determined as a function of excitation energy. This is shown in Fig. 3(b) for the energy range covered by our measurement.

3.1. Hyperdeformed transmission resonances in ^{236}U

The resonances at 5.27, 5.34 and 5.43 MeV had previously been identified as hyperdeformed resonances [3], however without resolving any rotational structure. For the first time, this was achieved in the present experiment. The resonance structure around 5.1 MeV excitation energy was formerly interpreted by Goldstone et al. [22] and Just et al. [13] as a vibrational resonance in the second minimum in analogy to the 5.1 MeV resonance in ^{240}Pu [20]. We will later interpret it as a group of hyperdeformed resonances.

The excitation energy region containing HD resonances was analyzed in two steps. We start with the resonance structure between 5.2 and 5.5 MeV, because here the hyperdeformed structure was already known [3], thus allowing for a test of our analysis procedure.

In order to describe the rotational structure, we assumed overlapping rotational bands with the same moment of inertia, inversion-splitting parameter and intensity ratio for the band members. Gaussians were used for describing the different band members. The relative excitation probabilities for the members of the rotational bands were taken from DWBA calculations for the (d, p) reaction by Back et al. [23], calculated around 5.4 MeV excitation energy for the upper and 5.1 MeV for the lower resonance region (see Table 1).

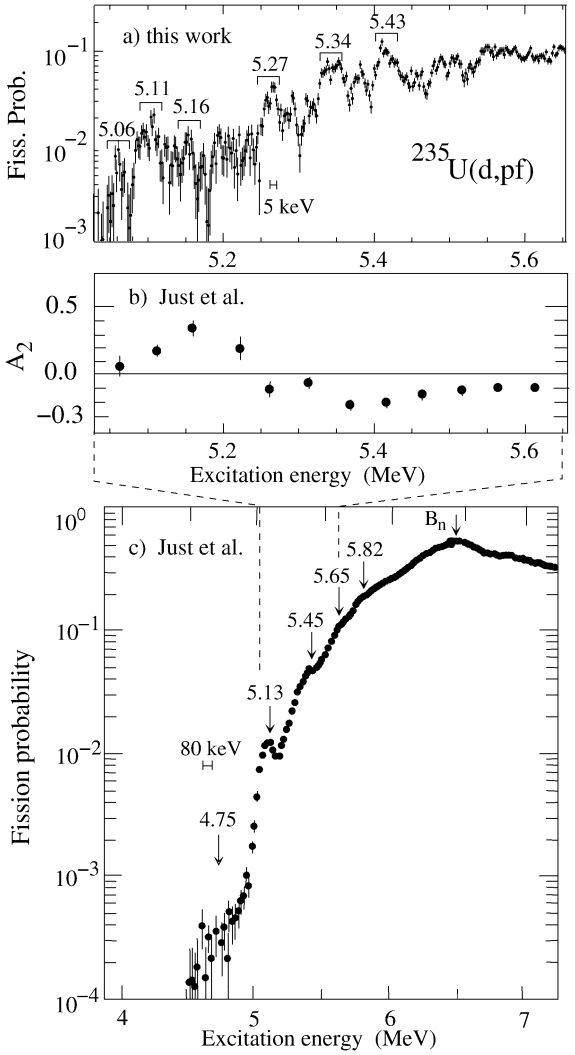

Fig. 3. (a) Prompt fission probability, P_f, for ^{235}U(d, pf) measured with high energy resolution in this work (random coincidences subtracted); (b) and (c): angular correlation coefficient A_2 for prompt fission following the reaction ^{235}U$(d, p)^{236}$U $\rightarrow f$ and prompt fission probability of ^{236}U from Just et al. [13]. The energy resolution of both measurements is indicated by a horizontal bar.

In case of the upper resonance region around 5.3 MeV an exponential background component was included in the fit procedure. In the lower resonance region only a negligible background contribution was identified. During the fitting procedure the energy of the band head and the absolute intensity of the band were used as free parameters. A common rotational parame-

Table 1
Relative excitation probabilities for rotational band members following ^{235}U(d, p) according to DWBA calculations by Back et al. [23] for $E^* = 5.1$ and 5.4 MeV

J	2		3		4		5		6		7	
π	−	+	−	+	−	+	−	+	−	+	−	+
Ref. [23] (5.4 MeV)	0.033	0.008	0.117	0.083	0.157	0.132	0.083	0.074	0.074	0.074	0.025	0.050
Ref. [23] (5.1 MeV)	0.050	0.008	0.121	0.059	0.150	0.100	0.096	0.075	0.092	0.058	0.025	0.058

ter ($\hbar^2/2\theta$) and inversion-splitting parameter ($\Delta E_\pm$) were adopted for each band.

The angular distribution of the fission fragments is defined by the total spin J and its projection K onto the deformation axis of the fissioning nucleus. The height of the outer fission barrier increases with increasing K value.

Since the ground-state spin and parity of the target is $\frac{7}{2}^-$, mainly $J^\pi = 3^-$ and $J^\pi = 4^-$ states are excited in the case of $l = 0$ transfer, in this way the fission barrier is relatively high. In the case of $l > 0$ transfer, the appearance of lower K values is also possible. Due to the limited energy resolution of the angular distribution measured by Just et al. [13], the A_2 angular correlation coefficients for states with different spins in a rotational band of a given K value cannot be extracted. Assuming an octupole rotational band with a certain K value, a theoretical A_2 coefficient was determined by averaging over the calculated $A(J, K)$ values weighted by the excitation probabilities for different J values taken from Ref. [23]. The calculated A_2 coefficients increase for $K \leqslant 3$, reaching a maximum at $K = 3$ before decreasing rapidly. At $K = 4$ a negative A_2 coefficient was obtained. Using the calculated $A_2(K)$ function, we derived the trend of the K values from the experimental A_2 coefficients as a function of the excitation energy. In this way we could determine the K values independently from fitting the fission probabilities.

The HD states are characterized by the presence of alternating parity bands with very large moments of inertia because of the very large quadrupole and octupole moments [11]. Assuming alternating parity bands with $J = K = 3$, 4 and 5 band heads, the fission probability between 5.2 and 5.5 MeV was fitted, resulting in the fit curve superimposed on the data in Fig. 4(a). The picket fence structures indicate the positions of the rotational band members, whilst the numbers to the left denote the corresponding K values which equal the lowest J value of the respective band. The corresponding normalized χ^2 values are presented in Fig. 4(c) as a function of $\hbar^2/2\theta$. The horizontal line represents the 99.9% (3σ) confidence level for the χ^2 test.

The deduced rotational parameter is $\hbar^2/2\theta = 2.3^{+0.3}_{-0.5}$ keV and for the inversion parameter a value of $\Delta E_\pm = 0^{+8.8}_{-5.5}$ keV was derived, which is consistent with the small inversion parameters obtained by Blons et al. [11].

Fitting the fission probability with rotational bands assuming a reversed parity assignment for the band members resulted in a fit of similar quality as the one shown in Fig. 4(a), thus indicating that the analysis is not sensitive to parity. In addition to the spin-dependent excitation probabilities of Back et al. also values calculated by Goerlach et al. [12] were used and found to produce almost identical results. Alternatively the assumption of a superdeformed rotational band structure was tested using spin sequences with $J = 2^+$, 4^+, 6^+ based on the same set of excitation probabilities as used for the HD bands. As shown by the dotted line in Fig. 4(c) no minimum for the normalized χ^2 was found in this case. With the series of 15 rotational bands shown in Fig. 4(a) not only the fission probability could be reproduced, but also the angular correlation coefficient A_2 measured by Just et al. [13] (data points in Fig. 4(c)) could be reproduced by bands with high K values ($K = 3$, 4 and 5, solid line in Fig. 4(b)). Again the assumption of SD rotational bands with $J = 2^+$, 4^+, 6^+ fails to reproduce the data, as indicated by the dashed line in Fig. 4(b).

The extracted rotational parameter corresponds to a value characterizing HD rotational resonances. The moment of inertia $\theta = 217 \pm 38\ \hbar^2/\text{MeV}$ is in good agreement with the values calculated by Shneidman et

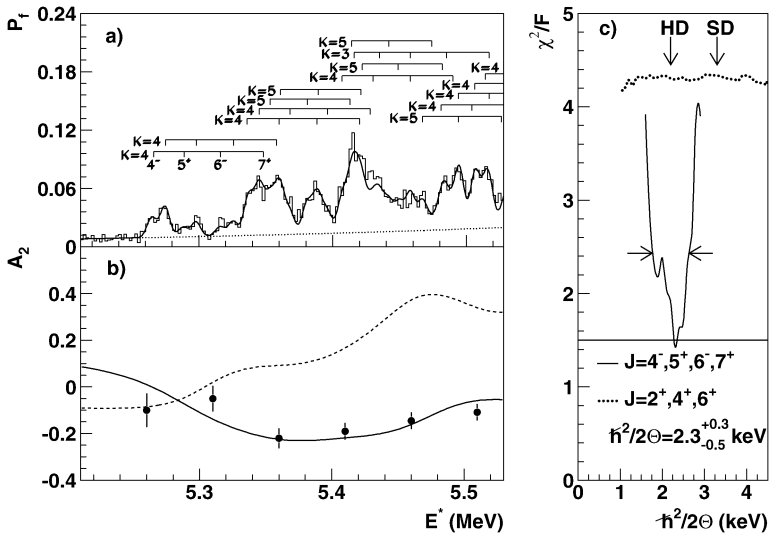

Fig. 4. (a) Fission probability (P_f) for the ^{235}U(d, pf) reaction in the excitation-energy region above 5.2 MeV. The solid line shows a fit to the data assuming alternating-parity rotational bands starting with $J = K$, the dotted line represents the exponential background component included in the fitting procedure. The picket fence structures indicate the positions of the rotational band members used in the fit with K values as indicated for each band by the left-sided numbers. (b) Angular-correlation coefficients A_2 from Ref. [13] (data points), superimposed by the A_2 coefficients inferred from the fit curve from a) (solid line). In addition the curve for $A_2(E^*)$ resulting from the assumption of superdeformed bands (dotted curve in (c)) is shown as a dashed line. (c) Normalized χ^2 values for the fit to the spectrum of panel (a)) (solid line). The dotted line represents the fit quality for the alternative scenario of superdeformed rotational bands. The best fit has been obtained by hyperdeformed rotational bands with $\hbar^2/2\theta = 2.3^{+0.3}_{-0.5}$ keV. The horizontal line represents the 99.9% (3σ) confidence level for the χ^2 test.

al. [24] for ^{234}U and ^{232}Th, who assumed dinuclear systems suggesting the possibility of an exotic heavy clustering as predicted by Ćwiok et al. [7].

In the second step of the analysis, the proton energy spectrum below 5.2 MeV was investigated, where so far no conclusive high-resolution data were available. In the ^{234}U(t, pf) reaction, Back et al. [25] observed a weak, narrow resonance at 5.0 MeV and a distinct shoulder (or resonance) around 5.15 MeV. Goldstone et al. [26] and Just et al. [13] reported the first clear observation of a series of narrow sub-barrier fission resonances in ^{236}U produced in the (d, pf) reaction. The measured resonance energies are given in Fig. 3(c). In their analysis the underlying states of these resonances were assumed to originate from the second well, close to the top of the inner barrier.

The result of the analysis in the excitation energy region between 5.05 and 5.2 MeV is shown in Fig. 5, where the prompt fission probability is displayed (panel (a)) together with the results of a fit by rotational bands similar to the procedure described above for the upper resonance region. Again the spin-dependent excitation probabilities of the rotational-band members were based on DWBA calculations by Back et al. [23] for $E^* = 5.1$ MeV.

In order to allow for a consistent description of the fission probability and the angular correlation coefficient A_2 from Just et al. [13], a distribution of K values rising from $K = 1$ to $K = 4$ between 5.05 and 5.2 MeV had to be chosen, thus differing from the excitation-energy region between 5.2 and 5.4 MeV discussed above, where higher K values were dominating.

Again the picket fence structures indicate the positions of the rotational band members, together with the K value of the corresponding band. While the fit of the fission probability showed little influence of the $J = 3$ rotational band members, a consistent description together with the angular correlation data required to include $J = 3$ with an intensity reduced by a factor of four with respect to the intensity listed in Table 1.

The sign change of the A_2 coefficient from negative values in the upper resonance region to largely positive values in the lower resonance region already indicates the tendency towards lower K values with decreasing excitation energy. The resulting curve for

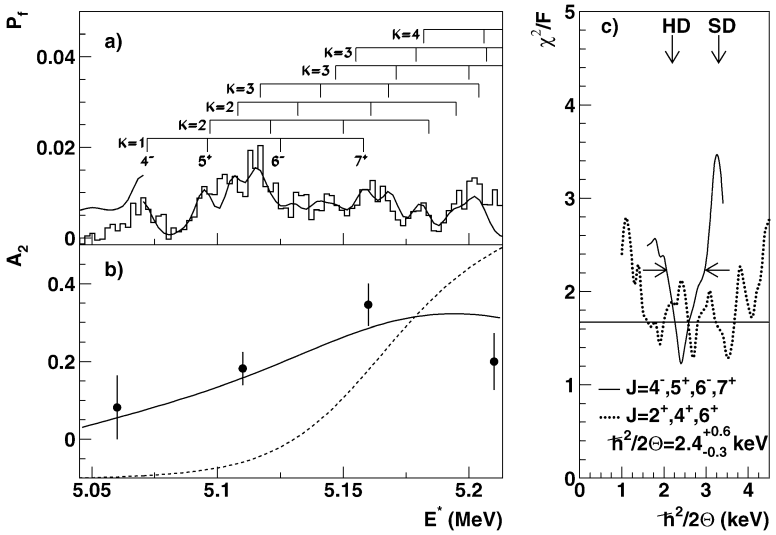

Fig. 5. (a) Fission probability (P_f) for the ^{235}U(d, pf) reaction in the excitation-energy region below 5.2 MeV. The superimposed solid line shows a fit to the data using rotational bands with a variable rotational constant $\hbar^2/2\theta$. The picket fences indicate the positions of the rotational band members, whilst the numbers to the left denote the K value of the corresponding band. In each case the band starts with a $J^\pi = 3^+$ member with reduced intensity (see text) and a dominant $J^\pi = 4^-$ state. The best fit has been obtained by using hyperdeformed rotational bands with a rotational parameter $\hbar^2/2\theta = 2.4^{+0.6}_{-0.3}$ keV, as indicated by the normalized χ^2 values shown in panel (c) (solid line). The horizontal line marks the 99.9% (3σ) confidence level of the χ^2 test. The dotted line in (c) shows the resulting fit quality under the assumption of a superdeformed spin sequence $J = 2^+, 4^+, 6^+$. (b) Angular-correlation coefficients A_2 from Ref. [13] (data points), reproduced by the A_2 coefficients inferred from the fit curve from (a). In addition the curve for $A_2(E^*)$ resulting from the assumption of superdeformed bands (dotted curve in (c)) is included as a dashed line.

the A_2 angular-correlation coefficient calculated based on the fit function derived from the fission probability in panel (a) is displayed as a solid line in panel (b) of Fig. 5. The quality of the fit can be judged from Fig. 5(c), where the normalized χ^2 values are displayed with the horizontal solid line representing the 99.9% confidence level.

The rotational parameter derived from the best fit (Fig. 5(c)) could be determined as $\hbar^2/2\theta = 2.4^{+0.6}_{-0.3}$ keV, corresponding to a hyperdeformed configuration. This result is in contrast to the old assumption that the decaying vibrational excitations originate from the superdeformed second minimum.

Assuming overlapping rotational bands in the second well with a spin sequence of $J^\pi = 2^+, 4^+, 6^+$ and using the same excitation probabilities from Back et al. [23] as before, the result of the χ^2 analysis is shown as a dotted line in panel (c) of Fig. 5. No unambiguous minimum for either HD or SD configurations was found. However, when comparing the corresponding curve for $A_2(E^*)$ (dotted line in Fig. 5(b) to the data points, a clear preference for HD configurations can be concluded. In the scenario of rotational bands with $J^\pi = 2^+, 4^+, 6^+$ a pronounced minimum of the normalized χ^2 at a value of the rotational constant $\hbar^2/2\theta \sim 3.3$ keV (typical for SD bands) could only be achieved by artificially increasing the 2^+ excitation probability by a factor of about 4, while again failing to reproduce the angular correlation data.

3.2. The depth of the third minimum in ^{236}U

Similar to our previous work on the ground state excitation energy in the third well of ^{234}U [27], the depth of the third well was determined by comparing the experimentally obtained level spacings of the $J = 5$ members of the rotational bands of Figs. 4(a) and 5(a) with the calculated ones using the back-shifted Fermi-gas description of the level density ρ as parametrized by Rauscher et al. [28], complemented by the K dependency as described by Bjørnholm et al. [29]:

$$\rho(U, K, J, \pi) = \frac{1}{2} \cdot F(U, J) \cdot \rho(U) \cdot G(K), \qquad (1)$$

where

$$\rho(U) = \frac{1}{\sqrt{2\pi}\cdot\sigma}\cdot\frac{\sqrt{\pi}}{12a^{1/4}}\cdot\frac{\exp(2\sqrt{aU})}{U^{5/4}},$$

$$F(U,J) = \frac{J+1}{2\sigma^2}\cdot\exp\left(\frac{-J(J+1)}{2\sigma^2}\right),$$

$$\sigma^2 = \frac{\theta_{\text{rigid}}}{\hbar^2}\sqrt{\frac{U}{a}} \quad \text{with } U = E-\delta,$$

$$G(K) = \frac{1}{K_0\sqrt{2\pi}}\cdot\exp\left(-\frac{K^2}{2K_0{}^2}\right). \tag{2}$$

Summing over all the allowed K values we get back the formula of Rauscher

$$\rho(U,J,\pi) = \sum_{K=-J}^{K=+J}\rho(U,J,K,\pi). \tag{3}$$

Thus the level density is dependent only on three parameters: the level density parameter a, the back-shift δ and the cutoff parameter K_0^2. According to Ref. [30] the parameter K_0^2 at an excitation energy of 5.2 MeV as obtained from fragment angular distributions for the ^{239}Pu(n,f) reaction is $K_0^2 = 27$. In Ref. [28] an excitation-energy dependent parameterization of the level density parameter a was given by fitting to experimental level density data (see Eq. (14) in Ref. [28]). The $C(Z,N)$ "microscopic correction" in this parameterization was taken from the calculations of Möller et al. [31]. The pairing gap Δ, which is related to the back-shift δ, was calculated from the differences in the binding energies of neighboring nuclei applying Eq. (19) in Ref. [28].

In order to determine the excitation energy E_{III} of the ground state in the third minimum, the excitation energy $U_{\text{III}} = E-\delta-E_{\text{III}}$ relative to the ground state in the third well was used in Eq. (2). Varying the value of E_{III}, the level spacings in the third well were calculated according to Eq. (2) and compared to our experimental data for the $J=5$ levels (circles and curve labeled 'Rauscher 1' in Fig. 6). Due to the K-selective filtering of the fission barrier the unobserved $J=5$ levels from $K>3$ (<4) in the low (high) resonance region has to be corrected for. Taking into account the $G(K)$ weighting factors from Eq. (1), corrected average level distances were derived from the experimental data points for the two resonance regions (triangles in Fig. 6). Varying the backshift δ in order to describe the level density in the third well, a value of

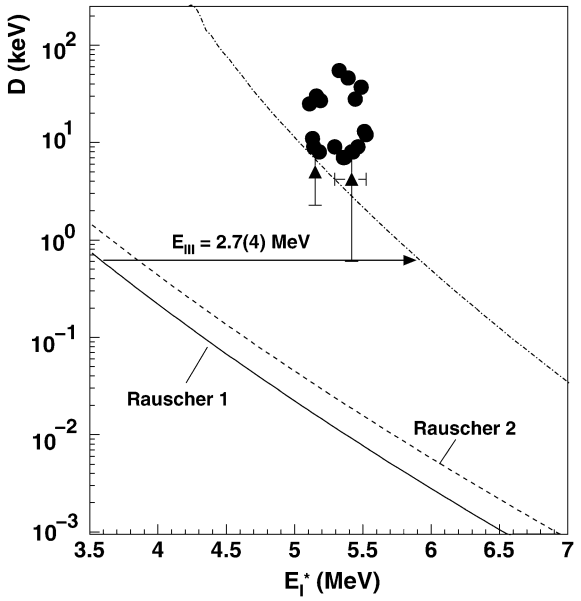

Fig. 6. Distances of the $J=5$ spin states in the third minimum of ^{236}U as a function of the excitation energy as derived from the fits in the two resonance regions discussed above. The solid curve ('Rauscher 1') shows values calculated by the parameterization of Rauscher et al. [28] (see text), the full points correspond to our experimental values. The dashed curve represents a calculation of the level density based on Eq. (2), using the experimentally determined value of the rotational constant instead of the rigid-rotor value. The triangles indicate the average level density in the two resonance regions, corrected for unobserved $J=5$ states due to the K-dependent filtering by the fission barrier. The dash-dotted curve originated from shifting the curve labeled 'Rauscher 1' through the corrected experimental level density data.

$E_{\text{III}} = 2.7$ MeV was determined (indicated by the arrow in Fig. 6).

From our fits to the fission probability we obtained a weighted average value of $\hbar^2/2\theta = 2.3\pm0.4$ MeV. Using this value instead of the rigid-rotor value for the determination of the spin-cutoff parameter σ in Eq. (2), we repeated the calculation of the level spacings (curve labeled 'Rauscher 2' in Fig. 6). In this case the analysis indicated a minimum at $E_{\text{III}} = 2.55$ MeV. Thus the uncertainty of E_{III}, composed of the uncertainty as obtained from our analysis and of the uncertainty introduced by the level density parameterization as quoted by the authors in Ref. [28], was estimated to be ±0.4 MeV.

Ćwiok et al. [7] predicted two different HD minima for U isotopes. In the case of ^{236}U, $E_{\text{III}} = 3.8$ MeV

corresponds to the less reflection-asymmetric HD minimum, while $E_{\mathrm{III}} = 2.4$ MeV belongs to the more reflection-asymmetric HD minimum. Our result is in good agreement with the prediction for the more reflection-asymmetric hyperdeformed minimum and with the so far only experimentally determined value of $E_{\mathrm{III}} = (3.1 \pm 0.4)$ MeV for ^{234}U as obtained in our previous work [27]. These two results represent the first experimental determination of the potential-energy landscape for hyperdeformed configurations.

3.3. The vibrational energy $\hbar\omega_{\mathrm{III}}$ in the third minimum

A further important quantity is the β-vibrational phonon energy in the third minimum. Looking at $\hbar\sqrt{C/B}$ with mass parameter B and stiffness C, from the oscillatory behaviour of B as a function of the deformation [32] a trend can be inferred indicating that B decreases from the second minimum to the third minimum to a value around the one known from the first minimum, whilst the potential gets softer (see Fig. 1) and C gets smaller. In this way a somewhat smaller value for $\hbar\omega$ compared to the second minimum of about 600 keV is expected for the third minimum.

In addition, there is the general feature that the fission probability of ^{234,236}U shows about twice as many resonances compared to the one for ^{240,238}Pu. This seems to be a general difference between the resonances in the second and the third minimum. Perhaps the spacing of these resonances can be explained by the fact that theoretically two hyperdeformed minima with $\beta_2 = 0.6$ but different β_3 values of 0.3 and 0.6 are predicted [7]. In this way in each minimum vibrational states with a spacing of about 0.5 MeV could occur, leading to a doubling of the number of resonances.

Compared to the situation in the second minimum of ^{240}Pu [20] transmission-resonance spectroscopy in the third well can be performed reaching down in energy to lower phonon numbers due to the thinner barriers and lower excitation energies within the third well.

3.4. The inner barrier of ^{236}U

The new interpretation of the 5.1 MeV transmission resonance in ^{236}U as a resonance in the third and not in the second minimum leads to a determination of the parameters of the inner barrier. Previously the interpretation as a resonance in the second minimum led to the requirement that the inner barrier height E_A was approximately equal to the outer barrier E_B, because a strong resonance requires penetrabilities of both barriers with comparable values [21]. Using our new interpretation the inner barrier has to be reduced to the excitation energy of the lowest transmission resonance in order to achieve a good mixing between the first and second minima.

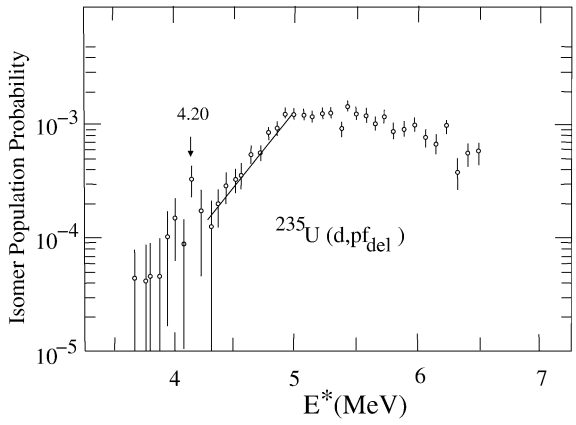

Fig. 7. Isomer population probability from Goerlach et al. [12,13].

With a back-shifted Fermi-gas formula the level spacing for 0^+ compound states in the second minimum at a total excitation energy of 5.1 MeV is calculated to be about 80 keV. The damping width of these states due to tunneling through the inner barrier $\Gamma = \hbar\omega_{\mathrm{II}}/2\pi \cdot P_A$ is about 100 keV at the top of the barrier with $P_A \approx 1$. Therefore the occurrence of a transmission resonance in the third well at 5.1 MeV requires a rather complete damping and an inner-barrier height E_A lower than 5.2 MeV. On the other hand, we can obtain a lower limit for the inner-barrier height E_A from the measurement of the isomer population probability. This is shown in Fig. 7 with data from Goerlach et al. [12,13]. For excitation energies between ~ 4.4 and ~ 4.9 MeV, the weak coupling limit is valid and the isomer population probability is proportional to the square root of the penetrability P_A of the inner barrier [33]. The data show a clear exponential increase. At an excitation energy of 5.1 MeV the isomer population probability starts to saturate because the compound states of the first and second minima become largely mixed. Above 6 MeV we observe a drop of the isomer population probability because the competing fission

and neutron channels open up. From the exponential rise of the isomer population probability for low energies we can deduce that the inner barrier E_A has to be larger than 4.9 MeV. From both limits we obtain $E_A = 5.05 \pm 0.20$ MeV. Furthermore, from the exponential rise and the estimate of the penetrability from the γ back-decay we obtain $\hbar\omega_A = 1.2$ MeV.

It is interesting to note that in the data of Goerlach et al. [12] in the very weak coupling region a resonance in the isomer population probability could be observed at an excitation energy of 4.20 ± 0.05 MeV (see Fig. 7). It nicely agrees with the sum of the isomer energy [34,35] and the energy of the second phonon $E_{\mathrm{II}} + 2 \cdot \hbar\omega_{\mathrm{II}} = (2.814 + 2 \times 0.685)$ MeV $=$ 4.184 MeV. This again shows that the second well at lower excitation energies is rather harmonic. A similar observation was made for the second well of ^{240}Pu [20]. The third phonon may be identified with the resonance observed in the prompt fission probability at 4.75 MeV (Fig. 3(c)). The energy of the fourth phonon may be reduced close to the top of the barrier E_A similar to the situation in ^{240}Pu [20]. In this way a vibrational enhancement of the coupling via the second minimum may occur for the 5.1 MeV resonance; but then the close-lying 5.27 MeV resonance would require a barrier energy below 5.27 MeV for complete damping. Allowing also for this special situation we have increased the error for determining the barrier $E_A = 5.05 \pm 0.2$ MeV.

3.5. The triple-humped fission barrier of ^{236}U

In Fig. 1 we showed to scale the triple-humped fission barrier of ^{236}U with our newly determined values. Significant information on the barriers is obtained also from the decay of the ground state of the second minimum. It has an excitation energy of 2814 ± 17 keV and a total half-life of 116 ± 3 ns [34,35]. The partial half-life for delayed fission is $t_{\mathrm{II}f} = 870 \pm 95$ ns and the partial half-life for the γ back-decay to the first minimum is $t_{\mathrm{II}\gamma} = 134 \pm 4$ ns. From the fission half-life the common penetrability of the outer two barriers $P_{B1} * P_{B2}$ can be calculated:

$$t_{\mathrm{II}f} = \frac{\ln 2 \cdot 2\pi\hbar}{\hbar\omega_{\mathrm{II}} \cdot P_{B1} \cdot P_{B2}}.$$

The β-vibrational phonon energy in the second minimum $\hbar\omega_{\mathrm{II}} = 685$ keV has been measured in conversion electron spectroscopy [36]. Thus we obtain: $P_{B1} \cdot P_{B2} = (4.5 \pm 0.4) \times 10^{-15}$. From the half-life of the γ back-decay we can deduce a rough estimate of the penetrability P_A of the inner barrier: $P_A = t_{\mathrm{I}\gamma}/t_{\mathrm{II}\gamma}$. The typical half-life $t_{\mathrm{I}\gamma}$ of the γ decay in the first minimum with an energy close to the isomer energy can be obtained from the Weisskopf estimate: $T_W(E1) = 6.76A^{-2/3}E_\gamma^{-3}$ [MeV] $\times 10^{-15}$ s combined with a typical Weisskopf hindrance factor $F_W = 100$ leading to: $t_{\mathrm{I}\gamma} \approx 10^{-15}$ s. In this way we obtain a penetrability of the inner barrier $P_A \approx 1 \times 10^{-8}$, which is about 7 orders of magnitude larger than the one of the two outer barriers.

For the inner barrier largely varying parameters have been published: ($E_A = 5.98 \pm 0.15$ MeV, $\hbar\omega_A = 1.32 \pm 0.1$ MeV [13,37]) or ($E_A = 5.6 \pm 0.2$ MeV, $\hbar\omega_A = 1.04$ MeV [4]). Here, we proved that a better choice of parameters is: ($E_A = 5.05 \pm 0.2$ MeV, $\hbar\omega_A = 1.2$ MeV) allowing for a full damping of the class-II compound states in the region where transmission resonances for the third minimum are observed.

From the saturation of the prompt fission probability an outer barrier height $E_B = 6.0 \pm 0.1$ MeV and a common curvature $\hbar\omega_B = 0.68 \pm 0.05$ MeV was deduced [13]. With these parameters we obtain a penetrability of the outer barrier of $P_B = 1.6 \times 10^{-13}$ at the excitation energy of the fission isomer. Adjusting the values within errors to $E_B = 6.1$ MeV and $\hbar\omega_B = 0.63$ MeV we obtain $P_B = 5.6 \times 10^{-15}$, in good agreement with the lifetime measurement. The strong occurrence of transmission resonances in the third minimum requires barriers B1 and B2 to have similar penetrabilities. Therefore, we have split the outer barrier into two symmetric barriers with the same height $E_{B1} = E_{B2} = 6.1$ MeV and curvatures $\hbar\omega_{B1} = \hbar\omega_{B2} = 2 \cdot \hbar\omega_B = 1.26$ MeV. The depth of the enclosed third minimum is $E_{\mathrm{III}} = 2.7 \pm 0.4$ MeV.

For the deformation of the second minimum a quadrupole moment $Q = (32 \pm 5)$ eb [38] was obtained, corresponding to an axis ratio of 1.9 ± 0.1. From the ground-state rotational band in the second minimum a rotational parameter $\hbar^2/2\theta_{\mathrm{II}} = 3.36 \pm 0.01$ keV [39] was determined. For the third minimum we obtained $\hbar^2/2 \cdot \theta_{\mathrm{III}} = 2.3 \pm 0.4$ keV as the weighted average of our two resonance regions. The barrier heights and the potential minima of Fig. 1 approximately agree with theoretically predicted values of $E_A = 5.46$ MeV, $E_{B1} = 6.0$ MeV, $E_{B2} =$

6.0 MeV, $E_{II} = 2.2$ MeV and $E_{III} = 3.8$ MeV from Ćwiok et al. [7] and Howard et al. [14].

4. Summary

In summary, we have measured the prompt fission probability of ^{236}U as a function of the excitation energy using the (d, pf) reaction with high resolution in order to study high-lying excited states in the third well. From the analysis of the rotational band structure in the two resonance regions around 5.1 and 5.3 MeV a weighted average for the rotational parameter could be extracted as $\hbar^2/2\theta = 2.3 \pm 0.4$ keV.

The corresponding moment of inertia ($\theta = 217 \pm 38\ \hbar^2$/MeV) agrees with the calculated value of Shneidman et al.. The hyperdeformed rotational-band structure observed in the rather low excitation energy region around 5.1 MeV independently supports our experimental finding of a rather deep third minimum, which is in agreement with theoretical predictions. We furthermore used the lowest transmission resonance in the third well to determine the height of the inner barrier $E_A = 5.05(20)$ MeV. In the double-humped barrier picture the inner barrier for light actinide nuclei always had to be adjusted above the highest observed resonance, while now the existence of a deep third minimum only requires that the inner barrier lies above the highest resonance in the second well. This represents a new trend in fission barriers for light actinides which is different from former assignments [4], but in good agreement with more recent theoretical predictions [14].

Acknowledgements

The work has been supported by DFG under HA 1101/6-3 and 436 UNG 113/129/0, the Hungarian Academy of Sciences under HA 1101/6-1, the Hungarian OTKA Foundation No. T038404.

References

[1] V. Metag, et al., Phys. Rep. 65 (1980) 1.
[2] P.G. Thirolf, D. Habs, Prog. Part. Nucl. Phys. 49 (2002) 245.
[3] A. Krasznahorkay, et al., Phys. Rev. Lett. 80 (1998) 2073.
[4] S.B. Bjørnholm, J.E. Lynn, Rev. Mod. Phys. 52 (1980) 725.
[5] P. Möller, J.R. Nix, in: Proceedings of the International Symposium on the Physics and Chemistry of Fission, Rochester, 1973, IAEA, Vienna, 1974, p. 103.
[6] P. Möller, et al., Phys. Lett. B 40 (1972) 329.
[7] S. Ćwiok, et al., Phys. Lett. B 322 (1994) 304.
[8] J. Blons, et al., Nucl. Phys. A 414 (1984) 1.
[9] J. Blons, Nucl. Phys. A 502 (1989) 121c.
[10] S. Bjørnholm, V.M. Strutinsky, Nucl. Phys. A 136 (1969) 1.
[11] J. Blons, et al., Nucl. Phys. A 477 (1988) 231.
[12] U. Goerlach, Diploma thesis, University of Heidelberg/MPI Heidelberg, 1978, unpublished.
[13] M. Just, et al., in: Proceedings of the International Symposium on the Physics and Chemistry of Fission, Jülich, 1979, IAEA, Vienna, 1979, p. 71.
[14] W.M. Howard, P. Möller, At. Data Nucl. Data Tables 25 (1980) 219.
[15] P. Ekström, http://nucleardata.nuclear.lu.se/database/masses.
[16] G. Audi, et al., Nucl. Phys. A 729 (2003) 1.
[17] A.H. Wapstra, G. Audi, C. Thibault, Nucl. Phys. A 729 (2003) 129.
[18] H.A. Enge, S.B. Kowalsky, in: Proceedings of the 3rd International Conference on Magnet Technology, Hamburg, 1970.
[19] H.F. Wirth, Ph.D. Thesis, TU Munich, 2001 http://tumb1.biblio.tu-muenchen.de/publ/diss/ph/2001/wirth.html.
[20] M. Hunyadi, et al., Phys. Lett. B 505 (2001) 27.
[21] A.V. Ignatyuk, N.S. Rabotnov, G.N. Smirenkin, Phys. Lett. B 29 (1969) 209.
[22] P.D. Goldstone, et al., Phys. Rev. C 18 (1978) 1706.
[23] B.B. Back, et al., Nucl. Phys. A 165 (1971) 449.
[24] T.M. Shneidman, et al., Nucl. Phys. A 671 (2000).
[25] B.B. Back, et al., Phys. Rev. C 9 (1974) 1924.
[26] P.D. Goldstone, et al., Phys. Rev. Lett. 35 (1975) 1141.
[27] A. Krasznahorkay, et al., Phys. Lett. B 461 (1999) 15.
[28] T. Rauscher, et al., Phys. Rev. C 56 (1997) 1613.
[29] S. Bjørnholm, A. Bohr, B. Mottelson, in: Proceedings of the International Symposium on the Physics and Chemistry of Fission, IAEA, Vienna, 1974, p. 367.
[30] R. Vandenbosch, J.R. Huizenga, Nuclear Fission, Academic Press, San Diego, 1973, p. 202.
[31] P. Möller, et al., At. Data Nucl. Data Tables 59 (1995) 185.
[32] T. Ledergerber, H.C. Pauli, Nucl. Phys. A 207 (1973) 1.
[33] U. Goerlach, et al., Z. Phys. A 287 (1978) 171.
[34] P. Reiter, Ph.D. Thesis, University of Heidelberg, 1993, MPI-H-V10-93.
[35] P. Reiter, et al., in: Yu. Oganessian, et al. (Eds.), Proceedings of the Conference on Low Energy Nuclear Dynamics, World Scientific, Singapore, 1995, p. 200.
[36] U. Goerlach, et al., Phys. Rev. Lett. 48 (1982) 1160.
[37] M. Just, Ph.D. Thesis, University of Heidelberg, 1978, unpublished.
[38] V. Metag, Habilitation thesis, Heidelberg, 1974.
[39] J. Borggreen, et al., Nucl. Phys. A 279 (1977) 189.